International Journal of Environmental Science and Technology (2023) 20:3749–3764
https://doi.org/10.1007/s13762-022-04226-4

ORIGINAL PAPER

Enhancing solar water heater system for utmost useful energy gain and reduction in greenhouse gas emissions in Gaza

M. Elnaggar[1] · H. J. El-Khozondar[2] · M. J. K. Bashir[3] · W. A. Salah[4]

Received: 5 July 2021 / Revised: 13 March 2022 / Accepted: 17 April 2022 / Published online: 10 May 2022

Abstract

Palestinians living in the Gaza Strip are in a very delicate situation when it comes to achieving sustainable growth in the energy sector, due to financial, environmental, and political challenges. Replacing electric water heaters with solar water heaters (SWH) in Gaza can lead to better hot water supply, cost savings, and gas emission reduction. Therefore, this study aims to improve the solar hot water system by determining the best values of tilt angle and incidence angle at which the useful energy obtained from a solar thermal collector has its optimum value. In addition, to evaluate the overall benefit of SWH in terms of cost savings from SWH replacement and reduction in greenhouse gas emissions which will provide useful information to investors and decision makers. Two software programs are used in the current study: The first software program is Transient System Simulation Tool which is used to calculate the useful solar energy obtained from the flat-plate collector and the second software is Design-Expert with response surface methodology which is utilized to obtain the optimal tilt angle. The simulation results show that the value of the useful energy gain of a solar thermal collector depends on the values of the tilt and incidence angles. The optimal value of the tilt angle is not fixed all over the year instead it has different values that are subject to the season or months of the year. The optimum value of incident angle is small and varies from 10 to 12°. The optimized tilt angles for Winter, Spring, Summer, and Autumn are 39.57°, 26.72°, 20.15°, and 32.2° and the maximum useful energy obtained with these angles are 225.69 kWh, 481.56 kWh, 599.40 kWh, and 386.19 kWh, respectively. The result exposes that the utilization of a standard solar water system can save up to $857.87 in energy cost per year. It was found that the payback period of the investment for a solar water heating system in Gaza is around 3.4 years. The results are promising and can motivate investors and decision makers to use SWH and solar energy.

Keywords Useful gained energy · Controlling angles · Cost saving, emission reduction · TRANSYS · Solar thermal collector

Editorial responsibility: Q. Aguilar-Virgen.

✉ H. J. El-Khozondar
hkhozondar@iugaza.edu

[1] Engineering Program Department, Palestine Technical College - Dier El-Balah, Gaza, Palestine

[2] Electrical Engineering and Smart Systems Department, Islamic University of Gaza, P. O. Box 108, Gaza, Palestine

[3] Department of Environmental Engineering, Faculty of Engineering and Green Technology (FEGT), Universiti Tunku Abdul Rahman, 31900 Kampar, Perak, Malaysia

[4] Department of Electrical Engineering, College of Engineering and Technology, Palestine Technical University - Kadoorie, Yafa Street, P.O. Box 7, Tulkarm, Palestine

List of symbols

A	Total collector array aperture or gross area (consistent with FR ($\tau\alpha$), FRUL, FRUL/T and Gtest) (m^2)
C_{pf}	Specific heat of collector fluid (kJ/kg-K)
F_R	Overall collector heat removal efficiency factor (–)
F'	Fin efficiency factor (–)
I	Global (total) horizontal radiation (kJ/h-m^2)
I_d	Diffuse horizontal radiation (kJ/h-m^2)
I_T	Global radiation incident on the solar collector (tilted surface) (kJ/h-m^2)
I_{bT}	Beam radiation incident on the solar collector (kJ/h-m^2)
$\dot{m}$	Flow rate at use conditions (kg/h)
$\dot{m}_{test}$	Flow rate in test conditions (kg/h)
N_G	Number of glass cover (–)
N_S	Number of identical collectors in series (–)

$\dot{Q}_u$	Useful energy gain (kJ) or (kWh)
T_a	Ambient (air). Temperature (°C)
T_{av}	Average collector fluid temperature (°C)
T_i	Inlet temperature of fluid to collector (°C)
T_o	Outlet temperature of fluid from collector (°C)
U_L	Overall thermal loss coefficient of the collector per unit area (kJ/h-m^2-K)
$U_{L/T}$	Thermal loss coefficient dependency on T (kJ/h-m^2-K^2)
W	Mean wind velocity (m/s)
α	Short-wave absorptance of the absorber plate (–)
β	Collector slope above the horizontal plane (tilt angle) (°)
θ	Incidence angle for beam radiation (°)
$(\tau\alpha)$	Product of the cover transmittance and the absorber absorptance (–)
$(\tau\alpha)_b$	(τα) For beam radiation (depends on the incidence angle θ) (–)
$(\tau\alpha)_n$	(τα) At normal incidence (–)
$(\tau\alpha)_s$	(τα) For sky diffuse radiation (–)
$(\tau\alpha)_g$	(τα) For ground reflected radiation (–)
T_p	The collector stagnation temperature (°C)
h_w	Convection coefficient of wind (W/m^2.K)

Introduction

Solar energy is an important source of sustainable and environmentally friendly energy (Salah et al. 2021a). There are various ways to benefit from solar energy (Elnaggar et al. 2019). Photovoltaic (PV) is the most common method of generating electricity from solar radiation. Different factors affect the amount of received solar irradiance at the collector surface, i.e., location, specific time and day of the year, tilt angle, and the angle of incidence of the solar radiation. Among these factors, the tilt angle is the most important because the correct choice of tilt angle enables the collector to receive the maximum amount of radiation (Handoyo et al. 2013). However, it is well-known that the overall efficiency of PV-based solar-power conversion is very low, and its enhancement is an ongoing research challenge. One way to tackle this issue is to use an integrated solar-thermal collector (PVT) to harness solar radiation to produce simultaneously electrical and thermal energy. Obviously, the PVT technique would be promising in locations where, in addition to electricity, there is a considerable scope for the direct thermal energy utilization such as water heating. Accordingly, the Gaza strip of Palestine has been chosen for the present research. Gaza Strip is exposed daily to an average solar ration of 6 kWh/m^2 at tilt angle of 31°. According to Palestinian households energy survey (July 2013), 62% of household in Palestinian are using solar energy for heating the water which is equivalent to 600 GWh annually (~ 100 million $) (Elnaggar et al. 2019).

In the literature, there are several studies dealing with the search for the optimal value of the tilt angle of PV systems. Hussein et al. (Hussein et al. 2004) investigate the effects of tilt angle and orientation of PV panels on the achievement of solar modules in Cairo, Egypt. Their result indicates that the maximum energy gained by PV panels occurs when the panels have tilt angle between 20 and 30° and facing the south direction. In addition, it is fine-tuned toward the west. Several studies have indicated the tilt angle substantial effect on the amount of received solar radiation (Hailu and Fung 2019; Jamil et al. 2016; Tang et al. 2009; Yunus Khan et al. 2020). Some studies suggested that the PV system tilt angle to be the same as the site latitude (Bari 2000; Benghanem 2011). In a study performed in Canada, researchers used isotropic and anisotropic diffuse sky radiation models to determine the optimum tilt angle (Hailu and Fung 2019). They recommended adapting the tilt angle value for four times a year to collect the most of solar radiation. In another study, researcher used automated solar water heating system to continuously provide hot water above a specific chosen temperature (Sadrin et al. 2009). The system works such that when the solar water heater failed to reach above the assigned temperature, the heating will be through the electric water heater. They claimed that the proposed system provides hot water using solar system 80% of the time and rest is covered by electric water heater.

In continuation of efforts for exploring green sources for power generation, Ampuno et al. (2021) studied solar parabolic thermal power generation plant model. The system is simulated using TRNSYS software and validated by MATLAB. The novelty of the work conducted by Ampuno et al. (2021) is the imitation of the entire solar collector model in terms of field and power conversion system which accomplished by enabling variation of outlet oil temperature and oil flow through decent valves. Their results showed a larger annual solar thermal energy of 2450 GJ obtained in island San Cristobal compared to 1080 GJ in Guayaquil and 1700 GJ in Manta.

The solar collectors optimum tilt angle differs at different geographical location due to longitude and latitude. All the related studies focused on areas such as Beirut (Lebanon) (Makarem et al. 2016; Sakkal et al. 1993), Surabaya (Indonesia) (Handoyo and Ichsani 2013), Cairo (Egypt) (Hussein et al. 2004), Toronto (Canada) (Hailu and Fung 2019), Malaysia (Bari 2000), Basrah (Iraq) (Saraf and Hamad 1988), Tabass (Iran) (Khorasanizadeh et al. 2014), Madinah (Saudi Arabia) (Benghanem 2011), and India (Jamil et al. 2016). Although the flat-plate solar-water heating system is used to heat water in Gaza Strip since a long time, there is a lack in studies that focus on determining the tilt angle optimal value. In previous studies, the optimal angles were determined as a function of the amount of solar radiation falling on the solar collector.

Accordingly, this study differs from previous studies by providing a comprehensive evaluation covers optimum energy gain, cost benefit, and environmental impacts from solar water heater at optimum conditions, in Palestine. To perform the calculation, two software programs are used to perform the simulation of the data which are Transient System Simulation Tool (TRNSYS) to calculate the useful solar energy obtained from the flat-plate collector and the Design-Expert software (DOE) with Response Surface Methodology (RSM) which is utilized to obtain the optimal tilt angle as mentioned in materials and methods section.Thus, this study aims to:

(1) Determine the optimal angles for the solar systems used in Gaza, Palestine, that produce maximum value of the useful energy gain (Q_u) through the solar collector. The present study pays attention for the losses through the collector from radiation such as collector, efficiency factor, and fin efficiency.
(2) Analyze the economic benefits and potential use of the investigated solar water heater in Gaza by considering greenhouse gases emission reduction, cost benefit analysis, and payback period. This information is equally important for public, investors, and decision makers.

Materials and methods

Location of current study

Gaza strip, Palestine, is chosen for the current study. Gaza Strip lays on the east of the Mediterranean coast with latitude of 31.5° N and longitude of 34.47° E (De Meij et al. 2016; Elnaggar et al. 2017). Figure 1 shows that during May, June, July, and August, the average sun radiation reaches Gaza by month is above 200 kWh/m^2.

Useful gained energy using flat-plate collector

In solar water heating, the solar thermal collector (heat exchanger) is the core of the system, which converts solar energy into internal energy of the transport layer (Demirbas 2005). In this study, a flat-plate collector with gross area (A_a) equals 5 m^2 was used. In order to calculate solar thermal collector efficiency (η), the Hottel-Whillier equation (Duffie and Beckman 2013) (Eq. 1) is used (Ji et al. 2014; TRNSYS16 2004).

$$\eta = \frac{Q_u}{AI_T} = \frac{\dot{m}C_{pf}\left(\dot{T}_o - T_i\right)}{AI_T} \tag{1}$$

where Q_u (kJ) is the usable energy gain, IT (kJ/h-m^2) is the global radiation incident on the titled solar collector, A (m^2) is the gross area of the collector, m^2 (kg/h) is the flow rate

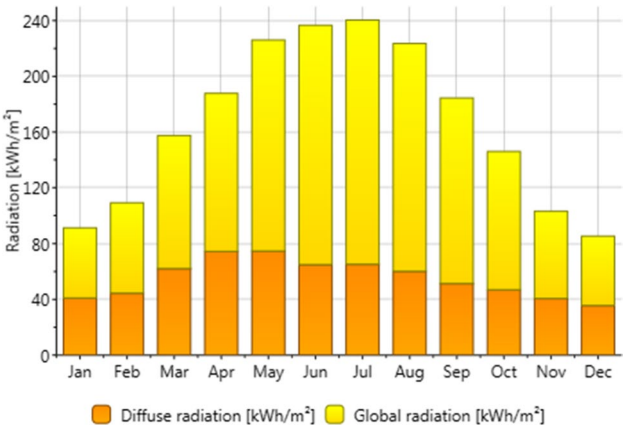

Fig. 1 Monthly average diffuse and global radiations for Gaza (Elnaggar et al. 2019)

under operating conditions, C_{pf} (kJ/kg-K) is the specific heat of the collector fluid, and To and Ti (°C) are the inlet and outlet temperatures of the fluid into the collector. In an array of a number of N_s modules, the energy of each module is represented by the Hottel-Whillier equation (Eq. 2) (TRNSYS16 2004):

$$\dot{Q}_u = \frac{A}{N_s}\sum_{j=1}^{N_s} F_{R\cdot j}\left(I_T(\tau\alpha) - U_{L\cdot j}\left(T_{i\cdot j} - T_a\right)\right) \tag{2}$$

where $\tau\alpha$ is the transmittance (τ)-absorptance (α) product, U_L is the overall heat loss coefficient, j is the module number, T_a (°C) is Ambient (air) temperature, and F_R is the collector heat removal factor defined as in Eq. 3.

$$F_{R,j} = \frac{N_s\dot{m}_c C_{pc}}{AU_{L,j}}\left(1 - \exp\left(-\frac{F'U_{L,j}A}{N_s\dot{m}_c C_{pc}}\right)\right) \tag{3}$$

where F' is the fin efficiency factor and C_{pc} is (kJ/kg-K) is specific heat of collector. The complexity of the loss coefficient ($U_{L,j}$) is due to its dependence on the collector construction and its operating conditions. An approximate value of $U_{L,j}$ (kJ/h-m^2-K) is given in Eq. 4 (Klein 1975):

$$U_{L,j} = \frac{3.6}{\frac{N_G}{\frac{C}{T_{P,j}}\left[\frac{\left(T_{avg}-T_a\right)}{N_G+F}\right]^{.33}+\frac{1}{h_w}}} + \frac{3.6\sigma\left(\left(T_{avg}^2 - T_a^2\right)\left(T_{avg} - T_a\right)\right)}{\frac{1}{\varepsilon p+.05N_G(1-\varepsilon p)} + \frac{2N_G+f-1}{\varepsilon g} - N_G} \tag{4}$$

where N_G is number of glass cover, T_{avg} is average collector fluid temperature, Convection coefficient of wind $h_w = 5.7 + 3.8$ W (W/m^2-K), W (m/s) is mean wind velocity, $f = (1 - 0.04\ h_w + 0.0005\ h_w^2)\ (1 + 0.091\ N_G)$ and $c = 365.9\ (1 - 0.00883\ \beta + 0.0001298\ \beta^2)$ where β is tilt angle. The value of $\tau\alpha$ is defined in Eq. 5.

$$\tau\alpha = \frac{I_{bT}(\tau\alpha)_b + Id\frac{(1+\cos\beta)}{2}(\tau\alpha)_s + \rho I\frac{(1-\cos\beta)}{2}(\tau\alpha)_g}{I_T} \quad (5)$$

where I_{bT} is beam radiation incident on the solar collector, I_d is diffuse horizontal radiation, I is global horizontal radiation, $(\tau\alpha)_s$, $(\tau\alpha)_b$, and $(\tau\alpha)_g$ are product for sky diffuse radiation, for beam radiation depending on the incidence angle θ, and for ground reflected radiation, respectively. Their values are found using function routine. The outlet temperature ($T_{o,j}$) of one module and the inlet to the next module ($T_{i,j}$) are given as:

$$T_{o,j} = \frac{AF_{R,j}\left(I_T(\tau\alpha) - U_{L,j}\left(T_{i,j} - T_a\right)\right)}{N_s\dot{m}_c C_{pc}} + T_i \quad (6)$$

When collector flow equals zero, the value of the collector stagnation temperature (T_p) is given in Eq. 7.

$$T_P = \frac{I_T(\tau\alpha)}{U_L} + T_a \quad (7)$$

For the definitions of all variables in Eqs. (1–7), please see Nomenclature table.

Solar thermal collector tilt angle

Figure 2 displays the parameters that affect the quantity of yearly solar radiation that hits the solar collector, i.e., the sun site in the sky. When the solar panel is horizontally placed (at $\beta = 0$), the incidence angle (θ) will equal the sun zenith angle (θz) which varies between 0 and 90°. At normal incidence, that is, the solar radiation strikes the surface of the solar panel at $\theta z = 0$, and solar panel will receive maximum amount of radiation. The tilt angle is an important parameter for acquiring the utmost solar radiation by solar panel which mainly relies on the location of the sun that varies daily, monthly, and yearly. To obtain maximum solar radiation, researchers try to optimize the values of tilt and incidence angle of solar collectors. For example, researchers work to minimize incidence angle of beam radiation by tracking the sun (Handoyo and Ichsani 2013; Yadav and Chandel 2013).

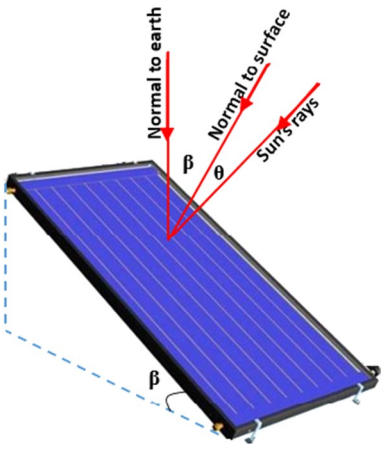

Fig. 2 Solar collector tilt angle (β) and the surface incidence angle (θ)

Modeling using TRNSYS

TRNSYS program to obtain the monthly maximum Q_u of the solar collector at different angles of inclination and incidence. The months of October, January, April, and July were selected to represent the seasons of Autumn, Winter, Spring, and Summer, respectively. The proposed solar-water-heating system model was analyzed using TRNSYS program, that is, a trustworthy tool used for solar energy applications. The designed model comprised three main parts: a storage tank, a flat-plate collector, and a pump. The TRNSYS model has the following components in its library (Fig. 3):

- Weather Data reading and processing (Type 109-TMY2)
- Flat-plate collector (Type 73) with total surface area of 5 m^2
- Storage tank (Type 4)
- Pump (Type 3b)
- Differential Controller w_Hysteresis (Type 2b)
- Plotter (Type 26)
- output\Printer (Type 25c)

Experimental layout and statistical analysis

The statistical analysis using DOE software is done using RSM which known for optimizing functioning parameters (Baş and Boyacı 2007; Elnaggar et al. 2013). RSM evaluates the dependence of the useful energy gain (Q_u) on the incidence and tilt angles. Moreover, it has been used to obtain the optimal values of the operating variables. The software DOE is used to determine the optimal value for the angle of inclination. Each independent variable (the angle of incidence (A) and the angle of inclination (B) were changed to three levels: low (− 1), medium (0), and high (+ 1), as shown in Fig. 4. The levels of the independent variables depend on the results of the first simulations.

Benefit analysis of SWH

Figure 5 shows a simple model developed particularly for the financial evaluation of solar water heating system. The model includes the key inputs for calculating the potential benefits of solar water heating system in Gaza, and employing this information to assess the cost, benefits, and the return of investment of SWH in Gaza. Table 1 presents the specification of SWH and energy benefits.

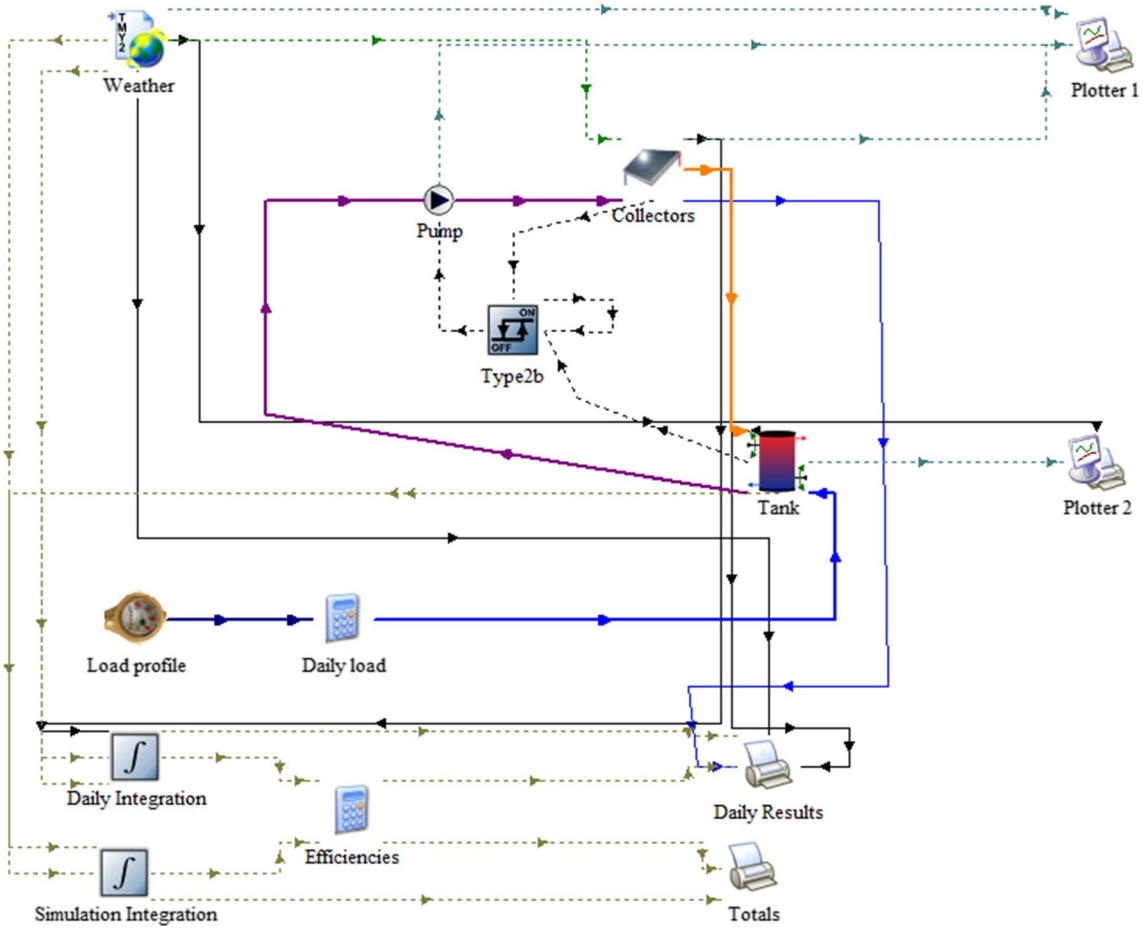

Fig. 3 TRNSYS model of solar water heating system (Extracted from TRNSYS software)

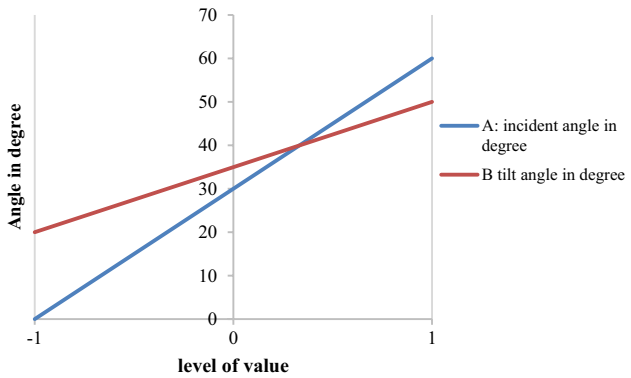

Fig. 4 Level of functional variables

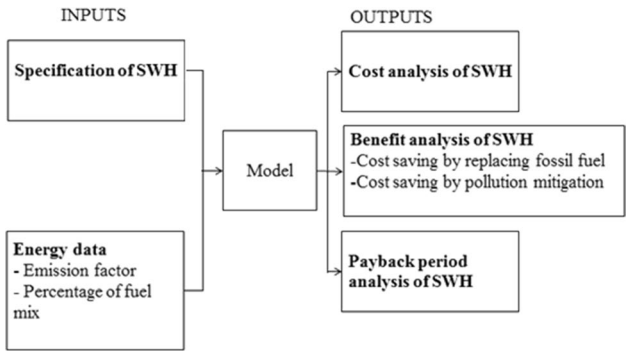

Fig. 5 Key information for modeling the cost–benefit, and payback period of a solar water heating system in Gaza

Pollutant emissions based on different energy sources

Table 2 exhibits the emission factors (indicators) of the individual energy sources as well as the measurement of the energy source in the electricity production mix in Palestine 2018. The emissions of air impurities resulted from the combustion of fossil fuels such as coal, oil, and natural gas for electricity generation depend primarily on the type of energy source used. It was reported that different sources contain different quantities of emissions or their mixtures (Saidur et al. 2007).

Table 1 Specification of SWH and energy benefit

Parameter	Unit	Value
Solar panel size	m^2	5
Tilt angle	degree	32
Average electricity consumption per capita	kWh/Yr/Capita	445.0
Electricity cost	$/kWh	0.17
Population of Gaza	Capita	2,000,000

Table 2 Air emission factors based on various energy sources. *Data sources*: (Jing et al. 2015)

Source of energy	Electricity production mix in 2018, (PE)%	Emission factor (EF) (10^{-3}) kg/kWh		
		CO_2	SO_2	NO_x
Coal	36.0	1180	13.9	5.2
Crude oil	10.0	850	16.4	2.5
Natural gas	54.0	530	0.5	0.9

The benefit was evaluated by considering the solar radiation in Palestine and energy harvesting by the proposed solar water heating system that comprises cost reduction and saving via replacing fossil fuels by renewal low-cost solar energy and emissions reduction.

Cost savings from replacing non renewable energy sources

Expenditure saving from replacing energy sources was projected based on the quantity of energy supplied and the associated costs. In this study, the energy replaced is electricity, and the unit price equals 0.17 $/kWh. The expenditure saved by replacing energy was computed using Eqs. 8 (Jing et al. 2015):

$$\mathrm{CBE} = \mathrm{BE} \times P \tag{8}$$

where BE = total energy cut, kWh; CBE = cost savings from switching energy source, $; P = unit price of switched energy, $/kWh.

Cost savings from pollution reduction

The cost that can be saved by reducing gas emissions can be estimated by the reduction in the amount of air pollutants emitted after the use of the solar boiler and the associated cost of treating these contaminants. Jing et al. (2015) highlighted that the expenses for treating 1000 kg of CO_2, NO_x and SO_x is approx. $ 20, $ 674.5, and $ 656.5, respectively. The cost conserving by gas emission reductions was assessed by Eq. 9–10:

$$\mathrm{BP}_{p,f} = \mathrm{BE} \times \mathrm{EF}_{p,f} \times \mathrm{PE}_f \tag{9}$$

$$\mathrm{CBP}_f = \sum_p \left(\mathrm{BP}_{p,f} \times \mathrm{TE}_p\right) \tag{10}$$

where $EF_{p,f}$ = emission factor of pollutant p by energy source f, kg/kWh; PE_f = percentage of energy source f in the energy mix; $BP_{p,f}$ = quantity of emissions p that are decreasing (e.g., CO_2, NO_x and SO_x) if solar. water heater avoids using electricity produced by energy source *f*, kg; CBP_f = *avoided cost of treating greenhouse gas and air pollutant emissions if* SWH avoids using electricity from combustible fuels *f*, $; TE_p = unit price of treating pollutant p, $/kg. The two values $EF_{p,f}$ and PE_p are given in Table 1.

Study to analyze the total cost of a solar water heating system

Because the economical profit of solar water heating system was valued every year, the necessary capital and operational costs were correspondingly anticipated per year for the payback analysis afterward. Table 3 presents the cost of solar water collectors in Gaza which was adopted in this study to estimate the potential saving once replaced the electric water heater.

Payback period analysis

The reimbursement duration is the period needed after using solar water heater to regain its financial investment. The payback period was calculated by looking into and comparing both annual cost and benefit over certain duration. In this study, the annual cost for each working year was assessed taking into consideration the capital and operatorial cost. Concerning the economic profit, it was evaluated mainly based on the energy cost saved per year.

Table 3 Cost of solar water Panel in Gaza

Description	Unit	Amount
Size of the solar panel	m^2	5
Total installation cost	$/Unit	2400
Maintenance cost	$/yr	150
Life period	yr	15

Results and discussion

Flat-plate collector useful gained energy

The assumed values of the flat-plate collector parameters (Fig. 6) are applied into the TRNSYS program such as the solar collector area is 5 m^2, collector fin efficiency factor of 88% and number of covers of 1.

Based on these parameters, TRNSYS program has been running, and each time the values of the functional parameters (A and B) are changed to get the Q_u by 5 m^2 area of flat-plate solar collector and data were recorded.

The months January, April, July, and October were selected to exemplify the seasons of the year Winter, Spring, Summer, and Autumn, respectively. The lowest useful energy was recorded in January, while the maximum useful energy was recorded in July. It is noted also from Fig. 7 that both angles have a noteworthy effect on harvesting the useful gained energy. In July, it is noticed that the value of Q_u increases with the decrease in the tilt and incidence angles, as the maximum value Q_u reaches 588.08 kWh at tilt angle and incidence angle of 20° and 0°, respectively, whereas in January, the value of Q_u increases with the increase in the tilt angle on condition of decrease in incidence angle as the highest value of Q_u in January equals 223.20 kWh at the tilt angle of 50° and the angle incidence angle of 0°. In April, the highest value of Q_u is 480.88 kWh at the tilt angle of 20° and the angle incidence angle of 0°. In October, the highest value of Q_u equals 485.49 kWh at the tilt angle of 35° and 0° incidence angle. In general, the smaller the incidence angle leads to increase useful energy in all months of the year, while the tilt angle varies in each month to obtain the largest useful energy. Therefore, to solve this entanglement and overlap, the authors used the DOE software tool with (RSM) to achieve the optimal tilt angles for each season of the year.

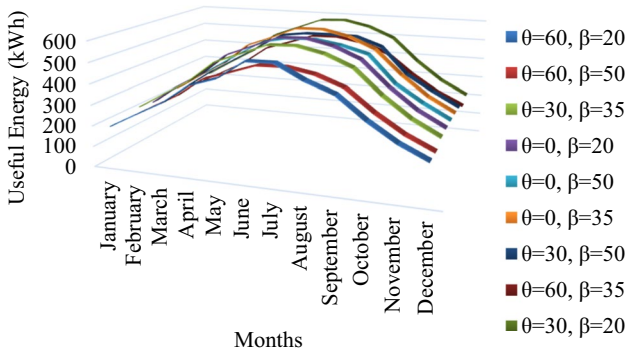

Fig. 7 Monthly average Q_u (kWh) at various vales of incidence and tilt angles

Analysis of variance (ANOVA)

Table 4 shows the analysis of variance of the regression parameters of the predictive quadratic response surface paradigm. As can be seen from Table 4, the F value of the model for Q_u of 32.77 means that the model is significant. For January, the *P*-value for the model is equal to 0.0001(<0.05) which shows the significance of the presented model terms. In the present case, the terms A, B, AB, A^2 and B^2 are the significant terms of model. Similarly, the models for Q_u calculations are repeated for April (Table 5), July (Table 6), and October (Table 7). As shown in Tables 5, 6 and 7, the *P*-values are also less than 0.05 which confirms that terms of model *A*, *B*, *AB*, A^2, and B^2 are also a significant term of the presented model. On the other hand, the *P*-values for the month of July are greater than 0.1, which mean that the model terms such as B^2 are not significant. Therefore, B^2 was excluded to obtain a better model for July.

In order to foresee the average monthly useful energy gain, the response surface model is created which has been considered feasible. The final regression models for each

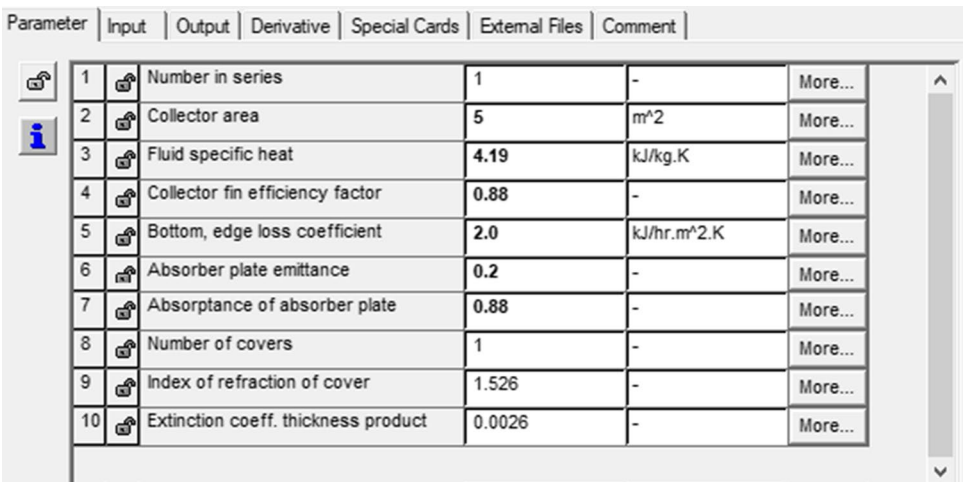

Fig. 6 Values of flat-plate collector parameters used to run TRNSYS software

Table 4 Winter ANOVA quadratic model

Source	Sum of squares	d_f	Mean square	*F*-value	*P*-value	
Block	62.11	1	62.11			
Model	1663.34	5	332.67	32.77	0.0001	Significant
A-incidence angle (θ in our model)	1043.23	1	1043.23	102.77	< 0.0001	
B-tilt angle (β in our model)	76.90	1	76.90	7.58	0.0791	
AB	56.25	1	56.25	5.54	0.0508	
A^2	332.33	1	332.33	32.74	0.0007	
B^2	56.57	1	56.57	5.57	0.0503	
Residual	71.06	7	10.15			
Lack of fit	71.02	3	23.67	2259.84	< 0.0001	Significant
Pure error	0.0419	4	0.0105			
Core total	1796.50	13				

Table 5 Spring ANOVA quadratic model

Source	Sum of squares	d_f	Mean square	*F*-value	*P*-value	
Block	134.73	1	134.73			
Model	6943.64	5	1388.73	75.14	< 0.0001	Significant
A-incidence angle	4329.72	1	4329.72	234.28	< 0.0001	
B-tilt angle	480.26	1	480.26	25.99	0.0014	
AB	149.88	1	149.88	8.11	0.0248	
A^2	984.67	1	984.67	53.28	0.0002	
B^2	325.23	1	325.23	17.60	0.0041	
Residual	129.37	7	18.48			
Lack of fit	129.37	3	43.12			
Pure error	0.0000	4	0.0000			
Cor total	7207.74	13				

Table 6 Summer ANOVA quadratic model

Source	Sum of squares	d_f	Mean square	*F*-value	*P*-value	
Block	3.59	1	3.59			
Model	8793.89	4	2198.47	22.11	0.0002	Significant
A-incidence angle	5049.89	1	5049.89	50.80	< 0.0001	
B-tilt angle	1972.00	1	1972.00	19.84	0.0021	
AB	67.18	1	67.18	6.758	0.0435	
A^2	1704.82	1	1704.82	17.15	0.0032	
Residual	795.33	8	99.42			
Lack of fit	795.33	4	198.83	5.965E + 08	< 0.0001	Significant
Pure error	1.333E-06	4	3.333E-07			
Cor total	9592.81	13				

winter, fall, spring, and summer are mathematically presented in the second-order polynomial in Eqs. (11, 12, 13, and 14), respectively.

$$Q_u = 186.9469 + 0.588048A + 1.69084B - 0.00833AB - 0.01227A^2 - 0.02024B^2 \quad (11)$$

$$Q_u = 455.0281 - 0.10478A + 2.39287B + 0.013603AB - 0.02111A^2 - 0.04853B^2 \quad (12)$$

$$Q_u = 610.4899 + 0.904408A - 0.93539B - 0.00911AB - 0.02588B^2 \quad (13)$$

Table 7 Autumn ANOVA quadratic model

Source	Sum of squares	d_f	Mean square	F-value	P-value	
Block	83.22	1	83.22			
Model	4705.21	5	941.04	123.82	< 0.0001	Significant
A-incidence angle	3295.43	1	3295.43	433.61	< 0.0001	
B-tilt angle	188.71	1	188.71	24.83	0.0016	
AB	49.80	1	49.80	6.55	0.0376	
A^2	681.69	1	681.69	89.70	< 0.0001	
B^2	123.60	1	123.60	16.26	0.0050	
Residual	53.20	7	7.60			
Lack of fit	53.20	3	17.73	5.320E + 07	< 0.0001	Significant
Pure error	1.333E-06	4	3.333E-07			
Cor total	4841.63	13				

$$Q_u = 369.162 - 0.00164A + 1.48526B - 0.0078411AB - 0.01757A^2 - 0.02992B^2 \quad (14)$$

where Q_u is useful energy gained by collector in kWh unit, A is incidence angle in degree unit and B is tilt angle in degree unit. The equations are expressed in terms of actual factors to see the direct relations between different factors and the useful gained energy and to forecast the response for specified altitudes of each factor.

Useful energy gained by the collector dependence on tilt and incidence angle

Equations 11, 12, 13, and 14 are numerically analyzed to envisage the effect of the operating variables which are the incidence and the tilt angles on the average monthly Q_u. The three-dimensional figures (Figs. 8, 9, 10 and 11) are the products of the DOE software tool with RSM, and they show the influence of the tilt angle (B) and incidence angle (A) on the useful energy gain (Q_u). Results clearly shown that a considerable effect on harvesting the useful energy gained from solar collector by the tilt and incidence angles.

The useful energy from the solar collector in January is shown in Fig. 8. The figure clarifies the effect of tilt and incidence angles on the useful energy from the solar collector in January that mainly representing the winter season. It is noticed from Fig. 8 that the useful energy increases when the angle of incidence ranges from 0° to 12°, after which the descent begins. In addition, the highest possible obtained energy during winter season reaches about 223.52 kWh for the tilt angle ranging between 32 and 50°.

Figure 9 displays the useful energy gained by solar collector as a function of tilt and incidence angles in April, which represents spring season. It is noticed from Fig. 9 that the useful energy increases when the incidence angle is less than

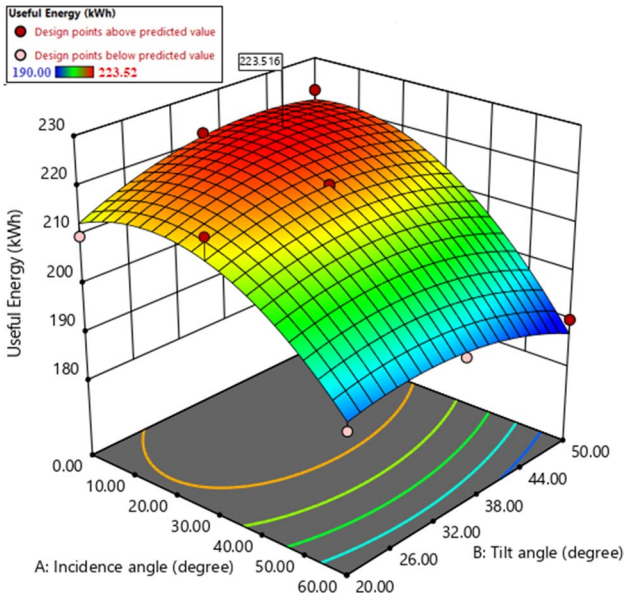

Fig. 8 Winter Q_u as a function of tilt and incidence angles

14°. For angles greater than 14°, the useful energy gained decreases. Meanwhile, during the spring season, it is found that the highest possible obtained energy reaches an about of 484.6 kWh at the tilt angle ranging between 0 and 32°.

July (which represents the summer season in this study) is one of the months with the highest useful energy of the year. This is because the sun is in the sky the most hours per day in July, reaching more than 13 h in Gaza. Moreover, the ambient temperature reaches 32 degrees, and the sky is clear and cloudless. As shown in Fig. 10, the useful energy obtained increases when the inclination and incidence angles decrease, since the maximum value of Qu reaches

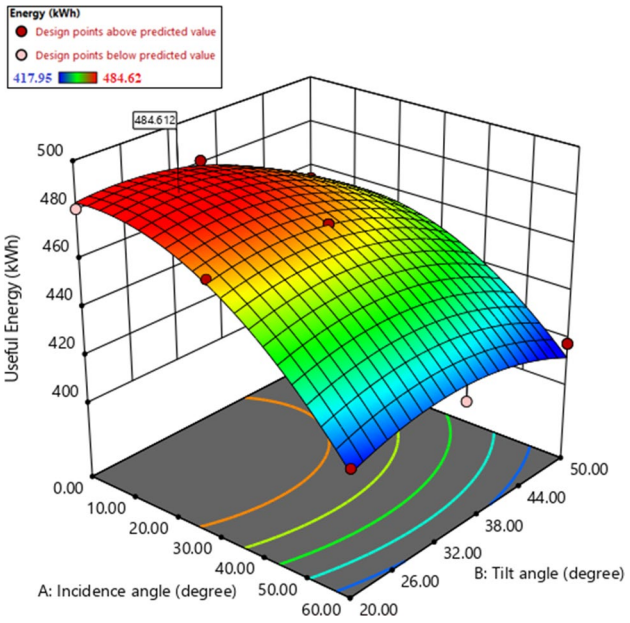

Fig. 9 Spring Q_u as a function of tilt and incidence angles

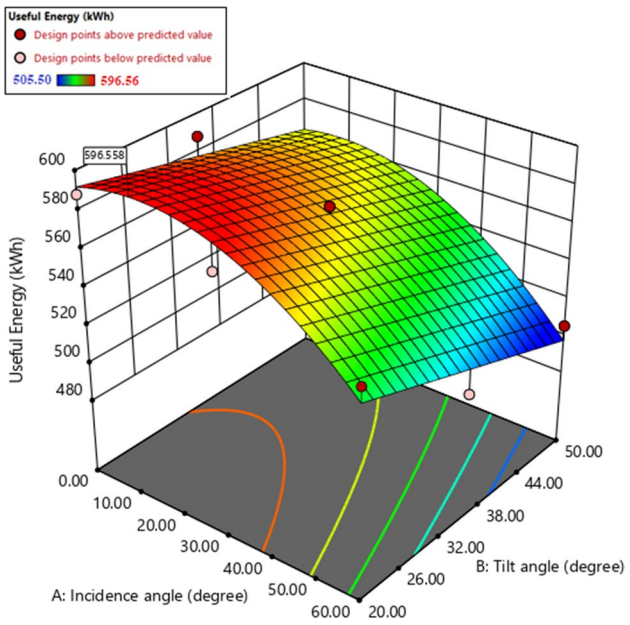

Fig. 10 Summer Q_u as a function of tilt and incidence angles

596.56 kWh when the inclination angle is 20°, and the incidence angle is less than 12°

Figure 11 shows the useful energy gained by solar collector as a function of tilt and incidence angles in October, which represents autumn season. Figure 11 shows that the

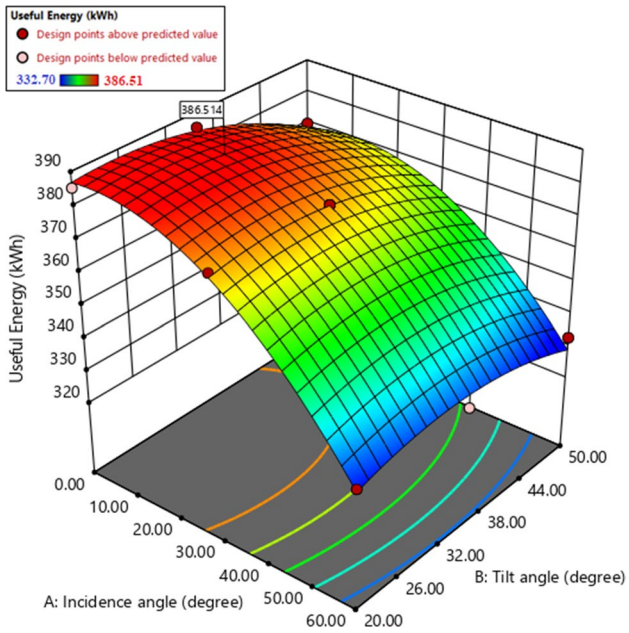

Fig. 11 Autumn Q_u as a function of tilt angle and incidence angles

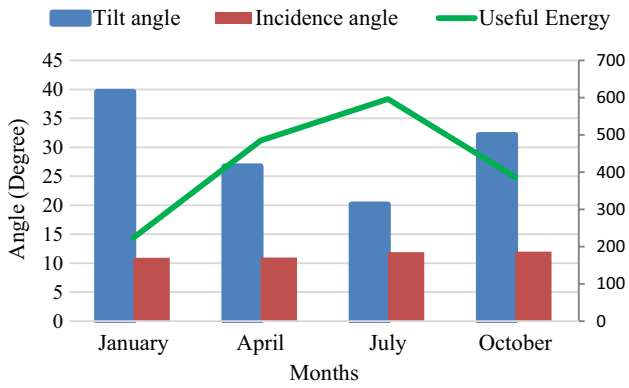

Fig. 12 Collector gained useful energy with the optimum incidence seasonal tilt and incidence angles

maximum useful energy gained at the incidence angle of 12° and the tilt angle of 32° reaches 386.51 kWh.

Optimization

For achieving the optimal tilt angle of the solar collector, DOE software with RSM, which is useful and dedicated tool, was used. To get accurate and realistic optimal tilt angle, the tilt angle is related to the incidence angle, and the optimum angles at which the maximum useful energy were

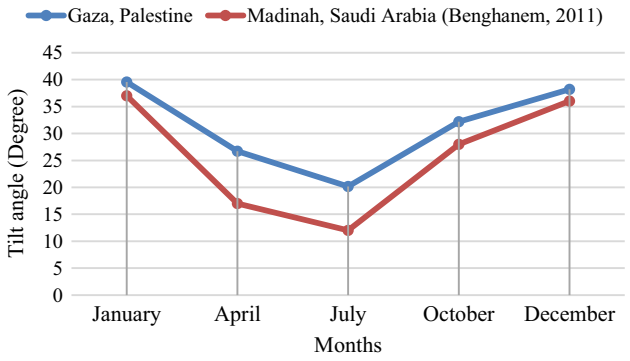

Fig. 13 Comparison between the values of optimal tilt angles between Gaza, Palestine and Madinah, Saudi Arabia

adopted. Figure 12 shows the tilt angles for the four seasons, respectively, and the maximum useful energy obtained. It is also noticeable from Fig. 12 that the optimum incidence angle is relatively stable during the seasons of the year, which are small values ranging from 10 to 12°.

Figure 12 displays that the values of the incidence angle is stable and small around 10–12° throughout the seasons to obtain the maximum useful energy. However, optimal tilt angles varies with seasons. It is found that in the summer season represented by the month of July in which it has a high temperature, the optimal tilt angle is small around 20°, whereas during the winter season represented by January where the temperature going low, the optimal tilt angle is relatively high around 39.57°.

Table 8 Daily average Q_u by flat-plate collector (5 m^2) at optimum tilt angle

Days	January θ=10.92°, β=39.57°		April θ=10.97°, β=26.72°		July θ=11.89°, β=20.15°		October θ=12°, β=32.2°	
	kJ	kWh	kJ	kWh	kJ	kWh	kJ	kWh
1	5559.997	1.5444	67,595.11	18.77642	78,587.3	21.8298	59,319.52	16.47764
2	20,005.68	5.557132	61,196.06	16.99891	78,092.8	21.69244	55,185.87	15.32941
3	28,292.38	7.858994	65,161.11	18.10031	73,757.68	20.48825	54,227.59	15.06322
4	25,981.66	7.217127	65,694.71	18.24853	71,047.84	19.73551	52,908.84	14.6969
5	25,488.24	7.080066	34,169.78	9.491604	76,848.22	21.34673	54,456.47	15.1268
6	30,994.42	8.60956	54,623.01	15.17306	71,852.7	19.95908	38,408.21	10.66895
7	30,598.3	8.499529	55,091.35	15.30315	77,344.41	21.48456	50,196.75	13.94354
8	20,651.98	5.736661	64,475.46	17.90985	73,009.99	20.28055	45,764.6	12.71239
9	22,586.71	6.274086	61,058.22	16.96062	75,500.81	20.97245	56,894.11	15.80392
10	34,610.44	9.614011	65,112.57	18.08682	70,533.67	19.59269	53,792.46	14.94235
11	21,541.37	5.983714	62,416.33	17.33787	69,996.88	19.44358	49,395.31	13.72092
12	29,629.26	8.230351	63,393.1	17.60919	75,032.22	20.84228	48,345.32	13.42926
13	21,499.2	5.972	59,170.99	16.43639	71,474.33	19.85398	49,862.46	13.85068
14	35,445.74	9.846038	40,176.26	11.16007	72,923.16	20.25643	46,326.63	12.86851
15	25,115.59	6.976552	55,524.9	15.42358	75,050.26	20.84729	22,785.42	6.329284
16	26,964.56	7.490155	53,503.41	14.86206	69,222.87	19.22857	46,696.66	12.9713
17	30,938.56	8.594043	63,920.71	17.75575	71,746.45	19.92957	39,303.13	10.91754
18	20,392.92	5.6647	43,694.35	12.13732	69,230.8	19.23078	51,678.71	14.3552
19	27,255.06	7.570851	64,956.53	18.04348	63,364.39	17.60122	45,781.65	12.71713
20	21,783.38	6.050939	50,512.75	14.03132	66,658.23	18.51618	43,495.98	12.08222
21	26,597.55	7.388208	56,931.78	15.81438	62,675.55	17.40987	50,671.12	14.07531
22	36,963.25	10.26757	63,021.85	17.50607	58,072.62	16.13128	45,922.36	12.75621
23	36,026.45	10.00735	46,160.82	12.82245	70,997.94	19.72165	50,041.86	13.90052
24	36,823.43	10.22873	58,032.67	16.12019	70,356.72	19.54353	42,456.63	11.79351
25	24,946.31	6.92953	56,937.77	15.81605	64,561.1	17.93364	45,501.51	12.63931
26	33,712.08	9.364466	62,141.26	17.26146	68,939.34	19.14982	46,755.09	12.98752
27	16,960.56	4.711268	54,149.81	15.04161	59,268.98	16.4636	43,598.55	12.11071
28	17,469.5	4.85264	56,201.41	15.6115	66,606.03	18.50168	41,937.08	11.64919
29	32,375.1	8.993082	59,719.91	16.58886	52,376.75	14.5491	30,711.74	8.531038
30	19,460.11	5.405587	68,859.69	19.12769	66,721.65	18.53379	27,859.51	7.738752
31	25,828.24	7.174512			73,186.18	20.32949		
Total	**812,498**	**225.69**	**1,733,604**	**481.56**	**2,157,837**	**599.40**	**1,390,281**	**386.19**

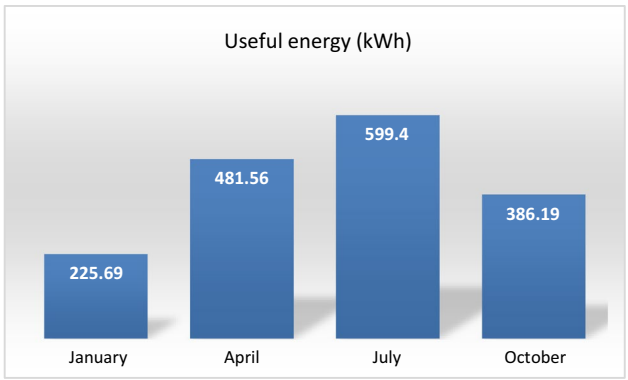

Fig. 14 Average monthly Q_u by the collector at optimum tilt angle for each season

A study compared the solar collector optimized tilt angle for Gaza city in Palestine with the same results for Madinah city in Saudi Arabia which is presented as shown in Fig. 13 (Benghanem 2011). The results had revealed that the tilt angle is homogeneous in both cities in all months. Furthermore, it is noted that the tilt angle for Gaza is slightly larger than the tilt angle for the city of Madinah. This is because the ambient temperature in Madinah city is higher than in Gaza city.

The daily average Q_u at the optimal tilt angle for January, April, July, and October is presented Table 8. It clearly noticed from the shown data that utmost useful energy is produced during July where its value can reach 21.83 kWh in the day. It also can be found from Table 8 that during the month of January, the harvested amount of useful energy is minimal.

Table 8 also reveals that the value of Q_u in the first day of January is the smallest and equals 1.544 kWh. This can be explained because the first day of January was rainy or cloudy, and the sun did not rise except for very limited periods. At the optimum tilt angle, the total of the daily Q_u by the collector for January, April, July, and October is 812,498 kJ (225.69 kWh), 1,733,604 kJ (481.56 kWh), 2,157,837 kJ (599.40 kWh), and 1,390,281 kJ (386.19 kWh), as shown in bold in Table 8 and Fig. 14.

Figure 15 displays the daily distribution of useful energy obtained from a flat-plate collector (5 m^2) at an optimal tilt angle for January, April, July, and October. Figure 15 is a graphical representation of the values presented in Table 6. It was observed that the useful energy of

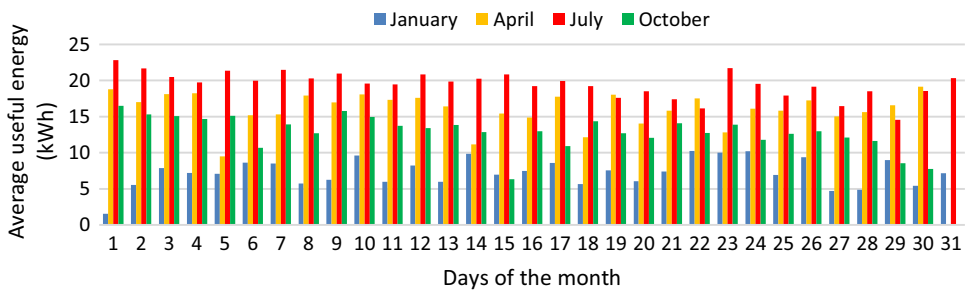

Fig. 15 Daily distribution of useful energy earned by flat-plate collector (5 m^2) at optimum tilt angle for January, April, July, and October

Table 9 Monthly average useful energy gained by flat-plate collector (5 m^2) for each optimum tilt angle

Months	θ=10.92°, β=39.57°		θ=10.97°, β=26.72°		θ=11.89°, β=20.15°		θ=12°, β=32.2°	
	kJ	kWh	kJ	kWh	kJ	kWh	kJ	kWh
January	812,484	**225.69**	792,396	220.11	777,816	216.06	799,956	222.21
February	1,112,796	309.11	1,087,596	302.11	973,212	270.34	1,100,160	305.6
March	1,359,972	377.77	1,355,760	376.60	1,401,782	389.38	1,357,884	377.19
April	1,713,384	475.94	1,733,616	**481.56**	1,733,504	481.53	1,729,512	480.42
May	1,913,652	531.57	1,913,004	531.39	2,017,852	560.51	1,916,604	532.39
June	2,002,320	556.20	2,098,548	582.93	2,116,066	587.79	2,107,908	585.53
July	2,016,576	560.16	2,117,088	588.08	2,157,836	**599.40**	2,116,764	587.99
August	1,948,212	541.17	2,015,568	559.88	1,999,995	555.55	2,013,912	559.42
September	1,815,804	504.39	1,818,108	505.03	1,642,853	456.35	1,816,704	504.64
October	1,340,028	372.23	1,387,116	385.31	1,389,201	385.89	1,390,280	**386.19**
November	1,036,836	288.01	1,032,156	286.71	919,641	255.45	1,035,288	287.58
December	785,232	218.12	778,536	216.26	758,927	210.81	783,756	217.71
Total	17,857,296	4960.36	18,129,492	5035.97	17,888,685	4969.08	18,168,728	5046.87

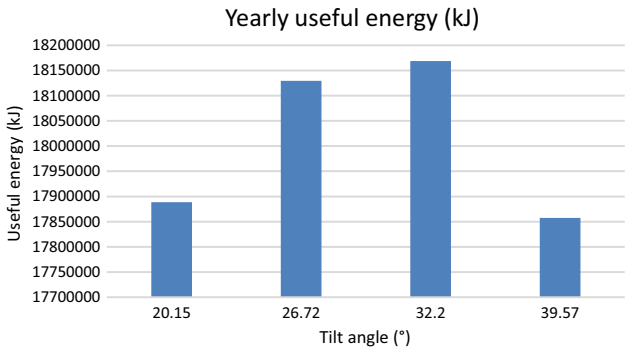

Fig. 16 Yearly useful energy gained by the collector for each optimum tilt angle in kJ

April exceeded that of July on the 29th day, which could be due to the difference in climate on that day in these two months.

The monthly average Q_u for each optimal tilt angle for all of the year is demonstrated as shown in Table 9. It clearly noticed from the obtained data that utmost useful energy in all of the year was produced at the optimal tilt angle of 32.2° where its value can reach 18,168,728 kJ/yr (5046.87 kWh/yr). The minimum value of the yearly useful energy was 17,857,296 kJ (4960.36 kWh) at the optimal tilt angle of 39.57°. The maximum values of the monthly average Q_u for each optimal tilt angle in kWh is shown in bold in Table 9.

Figure 16 shows the yearly useful energy gained by the collector for each optimum tilt angle where its value can reach 17,888,685 kJ, 18,129,492 kJ, 18,168,728 kJ, and 17,857,296 kJ at the optimum tilt angles of 20.15°, 26.72°, 32.2°, and 39.57°, respectively.

Benefit analysis of solar water heating system

The revenue of employing a solar water heating system was evaluated depending on the total quantity of energy that produced by SWH including profit by swapping energy sources and pollution reduction. It was found that each solar panel (5 m^2) has the capability to provide electricity to 12 capitals (heating water) continuously in Gaza and thus replace the dependency on the current non-renewable, non-reliable, and costly sources. Table 3 lists the solar panel cost and specification.

Cost saving by replacing energy source

In Gaza, nearly all of the building appliances consume electricity generated from non-renewable imported fossil fuels for operation (Salah et al. 2021b). By utilization of solar energy, reduction in energy cost, emission can be achieved. Cost saving by changing energy source was estimated by Pan et al. (2012), depending on the quantity of energy generated and its expenses once swap electricity with solar energy.

As given in Table 9, the useful energy of 5046.87 kWh/yr can be produced at the optimal tilt angle of 32.2°. It also can provide hot water to 12 persons. Consequently, a conventional solar water heater can avoid spending around $857.87 of energy fee per year, which is equal to $71.5 each month. This is a potential cost-effective benefit to the community, especially for low-income households, as it can reduce the financial inconvenience caused by electricity bills.

Table 10 Pollutant emissions reduction in Gaza per year per solar unit

Energy sources	Emission reduction (kg/yr)			Cost saving ($/yr)
	CO_2	SO_2	NO_x	
Coal	214.3	2.52	0.945	6.58
Crude oil	42.9	0.83	0.126	1.48
Gas	144.4	0.16	0.25	3.27
Total	401.6	3.51	1.32	11.33

Cost saving through air emissions reduction.

Since the solar water heater does not consume electrical energy for its daily operation, substituting electricity generated from fossil fuels with solar one will result in indirect reduction in the GHGs emissions (Jing et al. 2015; Salah et al. 2021a). Total expenses reduction due to the decrease in air pollutants emissions when consuming solar heater system and the expenses of treating those air impurities was assessed by Eq. 2 and Eq. 3. Table 2 introduces the emission factors of electricity production in Palestine and the share of each energy source in electricity production mix in 2018. As exemplified in Table 2, the emission factor for CO_2 from the main energy sources is considerably more than other impurities; this means that electricity generation generally releases more carbon dioxide than other pollutants. Hence, the use of solar energy has the highest CO_2 emission reduction followed by SO_2 and NO_x. Taking into consideration the approximate fee for treating 1 metric ton of CO_2, NO_x, and SO_2 as $20, $674.5, and $656.5, the expenses prevented due to the reduce in GHGs emissions are given in Table 10. As given in Table 10, each solar unit can help to avoid electricity power produced from fossil fuels can save $11.33 of treating cost per year.

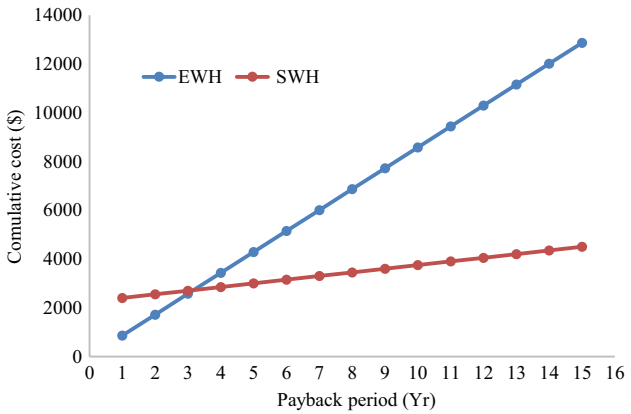

Fig. 17 Annual cost analysis for SWH versus EWH in Gaza

Cost analysis and payback period

The investment cost commonly consists of initial installation cost, operational cost including energy consumption, and maintenance expense. Solar water heating systems do not incur energy costs; therefore, the total investment cost is composed of the initial cost of the solar system installation and the maintenance cost (Ali et al. 2009). To ensure high productivity of SWH, solar heating systems need to be maintained once a year. Thus, it is important to determine the entire servicing and repairing cost for each year of operation. Figure 17 compares the cumulative costs of SWH versus EWH for 15 years. Solar water heaters which can be operated effectively for a longer duration have a lower annual cost than those operated for a shorter operating year. As longer operating interval means that the investment cost can be obtain back over longer period of time, it is crucial to ensure that the solar heating system can operate for as long as possible, or it will not be cost effective. In this research, the payback period of the investment for a SWH in Gaza was performed and reported. The economic benefits can recoup the relatively high initial investment cost for solar water heating system, through savings in electrical energy expenditures. Environmental benefit is not measured as a cost to the solar water heating system, as it is the funds reimbursed by the industry or government for treating those impurities discharged throughout electricity production. Normally, the payback period of the investment can be checked by comparing the costs and benefits of solar water heating systems. To calculate the payback period of the investment, the curves of annual cost and annual profit were constructed. The payback period of the investment corresponds to the working year in which the curves of annual cost and annual profit intersect. As shown in Fig. 17, the yearly cost of the solar water heater reduced considerably with the year of operation at the same time as the annual benefit increases with the year of operation; and the payback period is the year of operation in which the curves of year where the annual cost and annual benefit intersect. The estimated time for return of investment in a solar water heating system was 3.4 years.

Conclusion

The energy sector in Palestine is highly dependent on imports from other countries to meet the scarcity of energy supply, which mainly derived from fossil fuels. One possible alternative to reduce the use of fossil fuels utilization and ecological challenges is to use solar water heating systems instead of electric water heaters.

The effect of the title angle and incidence angle on the useful gained energy by PVT is studied and simulated for four seasons. Two programs are used to perform the simulations. The useful solar energy obtained by the flat-plate collector was calculated using TRNSYS program, while RSM was applied to optimize the tilt angle. In the study, the dependent variable is the useful energy, and the independent variables are the title and incidence angles. The study result indicates that both tilt and incidence angles are important factor that affect the maximum value of gained useful energy. It is also shown that optimal tilt angle changes its value according to the seasons and/or the months of the year. It is also found that incidence angle is hardly changes with seasons with small value that varies between 10 and 12° to obtain maximum gained useful energy. Though this occurs for small period of time, energy is gained during the rest of the day. But this work is concerned on maximum energy. The found maximum average useful values gained energy by PVT are 225.69 kWh, 481.56 kWh, 599.40 kWh, 386.19 kWh at optimal title angles values are 39.57°, 26.72°, 20.15°, and 32.2° for Winter, Spring, Summer, and Autumn, correspondingly. Also, the result exposes that the utilization of a standard solar water system can save up to $857.87 of energy cost per year. The payback on the investment in a solar water heating system in Gaza is 3.4 years. The results confirmed that replacing of electrical water heating system by solar water heating system is promising and in line with the United Nations Sustainable Development Goals as it can contribute to energy security, economic growth, and sustainable environment.

Supplementary Information The online version contains supplementary material available at https://doi.org/10.1007/s13762-022-04226-4.

Acknowledgements The authors would like to thank the Islamic Development Bank for supporting this research and the hosting institute "Islamic University of Gaza".

Author contributions ME collected data, designed and wrote most of the work; HJEK designed the work, write introduction, the methodology, analysis and conclusion; MJKB contributed by providing the mathematical modeling of the work and shared in writing and revising the manuscript; and WAS shared in writing and revising the manuscript. All authors approved the version to be published; and agreed to be accountable for all aspects of the work in ensuring that questions related to the accuracy or integrity of any part of the work are appropriately investigated and resolved.

Funding This work was supported by thank Islamic Development Bank [Grant numbers (2019-143526)] for academic year 2019–2020.

Data availability All information used are available in the text.

Code availability Transient System Simulation Tool (TRNSYS) and Design-Expert (DOE) tool.

Declarations

Conflict of interest The authors declare that they have no conflict of interest.

References

Ali B, Sopian K, Ghoul MA, Othman MY, Zaharim A, Razali AM (2009) Economics of domestic solar hot water heating systems in Malaysia. Eur J Sci Res 26(1):20–28

Ampuno G, Lata-García J, Jurado F (2021) Modeling of a solar thermal power generation plant for the coastal zones through the TRNSYS program. Electr Eng 103(1):125–137

Bari S (2000) Optimum slope angle and orientation of solar collectors for different periods of possible utilization. Energy Convers Manag 41(8):855–860

Baş D, Boyacı IH (2007) Modeling and optimization I: usability of response surface methodology. J Food Eng 78(3):836–845

Benghanem M (2011) Optimization of tilt angle for solar panel: case study for Madinah Saudi Arabia. Appl Energy 88(4):1427–1433

De Meij A, Vinuesa J-F, Maupas V, Waddle J, Price I, Yaseen B, Ismail A (2016) Wind energy resource mapping of Palestine. Renew Sustain Energy Rev 56:551–562

Demirbas A (2005) Potential applications of renewable energy sources, biomass combustion problems in boiler power systems and combustion related environmental issues. Prog Energy Combust Sci 31(2):171–192

Duffie JA, Beckman WA (2013) Solar engineering of thermal processes. Wiley, New York

Elnaggar MHA, Abdullah MZ, Mujeebu MA (2013) Experimental investigation and optimization of heat input and coolant velocity of finned twin U-shaped heat pipe for CPU cooling. Exp Tech 37(6):34–40

Elnaggar M, Edwan E, Ritter M (2017) Wind energy potential of Gaza using small wind turbines: a feasibility study. Energies 10(8):1229

Elnaggar M, Edwan E, Alnahhal M, Farag S, Samih S, Chaouki J (2019) Investigation of energy harvesting using solar water heating and photovoltaic systems for Gaza and Montreal QC climates. In 2019 IEEE 7th Palestinian international conference on electrical and computer engineering (PICECE). IEEE, pp 1–7

Hailu G, Fung AS (2019) Optimum tilt angle and orientation of photovoltaic thermal system for application in greater Toronto area. Can Sustain 11(22):6443

Handoyo EA, Ichsani D (2013) The optimal tilt angle of a solar collector. Energy Procedia 32:166–175

Hussein H, Ahmad G, El-Ghetany H (2004) Performance evaluation of photovoltaic modules at different tilt angles and orientations. Energy Convers Manag 45(15–16):2441–2452

Jamil B, Siddiqui AT, Akhtar N (2016) Estimation of solar radiation and optimum tilt angles for south-facing surfaces in humid subtropical climatic region of India. Eng Sci Technol Int J 19(4):1826–1835

Ji J, Wang Y, Yuan W, Sun W, He W, Guo C (2014) Experimental comparison of two PV direct-coupled solar water heating systems with the traditional system. Appl Energy 136(Supplement C):110–118

Jing OL, Bashir MJK, Kao J-J (2015) Solar radiation based benefit and cost evaluation for solar water heater expansion in Malaysia. Renew Sustain Energy Rev 48:328–335

Khorasanizadeh H, Mohammadi K, Mostafaeipour A (2014) Establishing a diffuse solar radiation model for determining the optimum tilt angle of solar surfaces in Tabass. Iran Energy Convers Manag 78:805–814

Klein S (1975) Calculation of flat-plate collector loss coefficients. Sol Energy 17:79

Makarem S, Ghali K, Ghaddar N, Karaki S (2016) Photovoltaic-thermal (PV/t) panel to minimize electrical and air conditioning energy consumption of a typical office in Beirut. Int J Green Energy 13(4):383–394

Pan TC, Kao JJ, Wong CP (2012) Effective solar radiation based benefit and cost analyses for solar water heater development in Taiwan. Renew Sustain Energy Rev 16(4):1874–1882

Sadrin S, Hossain M, Mohith E (2009) Alternative solar water heater for domestic purpose. BRAC University, Dhaka

Saidur R, Masjuki HH, Jamaluddin MY, Ahmed S (2007) Energy and associated greenhouse gas emissions from household appliances in Malaysia. Energy Policy 35(3):1648–1657

Sakkal F, Ghaddar N, Diab J (1993) Solar collectors for the Beirut climate. Appl Energy 45(4):313–325

Salah WA, Abuhelwa M, Bashir MJK (2021a) The key role of sustainable renewable energy technologies in facing shortage of energy supplies in Palestine: current practice and future potential. J Clean Prod 293:125348. https://doi.org/10.1016/j.jclepro.2020.125348

Salah WA, Abuhelwa M, Bashir MJK (2021b) Overview on the current practices and future potential of bioenergy use in Palestine. Biofuels Bioprod Biorefin 15(4):1095–1109

Saraf G, Hamad FAW (1988) Optimum tilt angle for a flat plate solar collector. Energy Convers Manag 28(2):185–191

Tang R, Gao W, Yu Y, Chen H (2009) Optimal tilt-angles of all-glass evacuated tube solar collectors. Energy 34(9):1387–1395

TRNSYS16, 2004. A transient system simulation program. User's manual solar energy laboratory, TRNSYS 16th edn. Solar Energy Laboratory, University of Wisconsin, Madison

Yadav AK, Chandel SS (2013) Tilt angle optimization to maximize incident solar radiation: a review. Renew Sustain Energy Rev 23:503–513

Yunus Khan TM, Soudagar MEM, Kanchan M, Afzal A, Banapurmath NR, Akram N, Mane SD, Shahapurkar K (2020) Optimum location and influence of tilt angle on performance of solar PV panels. J Therm Anal Calorim 141(1):511–532